# Predicting Humoral Alloimmunity from Differences in Donor and Recipient HLA Surface Electrostatic Potential

**Dermot H. Mallon,[*,†,‡] Christiane Kling,[§] Matthew Robb,[¶] Eva Ellinghaus,[‖] J. Andrew Bradley,[*,†,‡] Craig J. Taylor,[‡,#] Dieter Kabelitz,[§] and Vasilis Kosmoliaptsis[*,†,‡]**

**In transplantation, development of humoral alloimmunity against donor HLA is a major cause of organ transplant failure, but our ability to assess the immunological risk associated with a potential donor–recipient HLA combination is limited. We hypothesized that the capacity of donor HLA to induce a specific alloantibody response depends on their structural and physicochemical dissimilarity compared with recipient HLA. To test this hypothesis, we first developed a novel computational scoring system that enables quantitative assessment of surface electrostatic potential differences between donor and recipient HLA molecules at the tertiary structure level [three-dimensional electrostatic mismatch score (EMS-3D)]. We then examined humoral alloimmune responses in healthy females subjected to a standardized injection of donor lymphocytes from their male partner. This analysis showed a strong association between the EMS-3D of donor HLA and donor-specific alloantibody development; this relationship was strongest for HLA-DQ alloantigens. In the clinical transplantation setting, the immunogenic potential of HLA-DRB1 and -DQ mismatches expressed on donor kidneys, as assessed by their EMS-3D, was an independent predictor of development of donor-specific alloantibody after graft failure. Collectively, these findings demonstrate the translational potential of our approach to improve immunological risk assessment and to decrease the burden of humoral alloimmunity in organ transplantation.** ***The Journal of Immunology*****, 2018, 201: 3780–3792.**

The HLA gene complex encodes highly polymorphic proteins that are the main immunological barrier to successful cell, tissue, and organ transplantation. Immune recognition of HLA class I and class II expressed on donor tissue stimulate the development of donor-specific Abs (DSA) that are the major cause of organ transplant failure in the medium to long term (1–5). Moreover, development of alloantibody through pregnancy, blood transfusion, and previous transplantation may severely limit the opportunity for organ transplantation (6, 7). Current strategies to offset the risk for development of DSA and of Ab-mediated rejection focus on minimizing the number of HLA mismatches between donor and recipient and on the administration of immunosuppression regimens that aim to suppress the recipient immune response. HLA matching is incorporated into many deceased donor organ allocation schemes, but because of the extensive polymorphism of the HLA system and the relative limitation in the size of the donor organ pool, most recipients receive allografts with one or more mismatched HLA alleles. HLA-incompatible allografts necessitate the use of increased immunosuppression, and this is a major cause of recipient morbidity and mortality (8, 9).

Current assessment of the immunological risk associated with a particular transplant is based on enumerating the number of HLA mismatches between donor and recipient and is predicated on the assumption that all mismatches within an HLA locus are of equal significance to graft outcomes. However, it is clear from animal studies that humoral alloimmunity is critically dependent on the nature of the MHC mismatch between donor and recipient, and this has been supported by observational studies in humans, suggesting that certain donor HLA are tolerated by the recipient immune

*Department of Surgery, University of Cambridge, Addenbrooke's Hospital, Cambridge CB2 0QQ, United Kingdom; [†]National Institute for Health Research Blood and Transplant Research Unit in Organ Donation and Transplantation, University of Cambridge, Cambridge CB2 0QQ, United Kingdom; [‡]National Institute of Health Research Cambridge Biomedical Research Centre, Cambridge CB2 0QQ, United Kingdom; [§]Institute for Immunology, University Medical Centre Schleswig-Holstein, Kiel University, 24105 Kiel, Germany; [¶]Statistics and Clinical Studies Unit, National Health Service Blood and Transplant, Bristol BS34 7QH, United Kingdom; [‖]Institute of Clinical Molecular Biology, University Medical Centre Schleswig-Holstein, Kiel University, 24105 Kiel, Germany; and [#]Tissue Typing Laboratory, Cambridge University Hospitals National Health Service Foundation Trust, Cambridge CB2 0QQ, United Kingdom

ORCIDs: 0000-0001-7434-1201 (D.H.M.); 0000-0002-8809-9708 (C.K.); 0000-0003-2914-3382 (E.E.); 0000-0001-7298-1387 (V.K.).

Received for publication May 17, 2018. Accepted for publication October 2, 2018.

This work was supported by the Cambridge National Institute for Health Research (NIHR) Biomedical Research Centre and the NIHR Blood and Transplant Research Unit in Organ Donation and Transplantation at the University of Cambridge in collaboration with Newcastle University and in partnership with National Health Service Blood and Transplant. V.K. was supported by an Academy of Medical Sciences grant, an Evelyn Trust grant, and NIHR Post-Doctoral Fellowship PDF-2016-09-065. D.H.M. was supported by a Royal College of Surgeons of England research fellowship. This work was supported by an intramural research grant from Kiel University medical faculty (to C.K.) and Deutsche Forschungsgemeinschaft Grant KA 502/18-1 (to D.K.).

V.K., C.K., and D.K. conceived of the research idea and designed the research study. D.H.M., C.K., and V.K. conducted the experiments and acquired data. D.H.M., V.K., and M.R. analyzed the data. M.R. performed all statistical analyses. E.E. performed the HLA typing for the lymphocyte immunotherapy cohort. V.K., C.J.T., and J.A.B. conceived the research program and provided input into design and the analysis plan. D.H.M. and V.K. authored the manuscript. All coauthors provided review and revisions to the manuscript and ultimately approved the final version for submission and publication.

The views expressed are those of the authors and not necessarily those of the National Health Service, the Cambridge National Institute for Health Research, the Department of Health, or National Health Service Blood and Transplant.

Address correspondence and reprint requests to Dr. Vasilis Kosmoliaptsis, Department of Surgery, University of Cambridge, Addenbrooke's Hospital, Hills Road, Cambridge CB2 0QQ, U.K. E-mail address: vk256@cam.ac.uk

The online version of this article contains supplemental material.

Abbreviations used in this article: CI, confidence interval; 3D, three-dimensional; DSA, donor-specific Ab; EMS-3D, three-dimensional electrostatic mismatch score; ESD, electrostatic similarity distance; IQR, interquartile range; LIT, lymphocyte immunotherapy; MFI, mean fluorescence intensity; OR, odds ratio; PDB, Protein Data Bank.

system (10, 11). Recent evidence shows that the potential of donor HLA to induce humoral alloresponses (HLA immunogenicity) might be a function of the number and location of amino acid sequence polymorphisms compared with recipient HLA molecules (12, 13). Numerous studies support an association between donor HLA immunogenicity, considered at the amino acid sequence level, and the likelihood of DSA developing after transplantation, and that this approach might offer superior assessment of donor–recipient histocompatibility compared with conventional HLA-matching strategies (14–17). Studies by our group have shown that the predictive ability of sequence-based HLA immunogenicity algorithms can be significantly enhanced by consideration of the physicochemical properties of amino acid polymorphisms expressed on donor HLA molecules (18–21).

Despite its promise, sequence-based assessment of HLA immunogenicity does not account for the conformational nature of antigenic recognition by BCR and for the effect of individual amino acid polymorphisms on B cell epitope structure and physicochemical properties (e.g., surface exposure, polarity, surface charge, hydrophobicity) (22–24). In particular, Ab–Ag interactions are largely governed by electrostatic forces dictated by the number and distribution of charged atoms on the surface of the HLA molecule (24–27). We have previously shown that, despite variation in their amino acid composition, HLA B cell epitopes are characterized by unique surface electrostatic potential properties that explain serological patterns of HLA-specific Ab binding (28–30). In this study, we hypothesized that the capacity of donor HLA to induce a specific alloantibody response can be predicted by quantitative assessment of their structural and surface electrostatic potential differences compared with recipient HLA molecules. We have developed a novel computational scoring system to quantify and compare HLA electrostatic properties that uses molecular modeling techniques, structural information from x-ray crystallography, and application of protein electrostatics theory. This approach was validated by analysis of HLA-specific Ab responses in a unique model of HLA sensitization comprising patients that underwent a single injection of donor lymphocytes [lymphocyte immunotherapy (LIT)] in a defined donor–recipient setting without the influence of immunosuppression or interference from other sensitizing events. The applicability of our findings in transplantation was then examined by analysis of DSA responses in patients listed for repeat renal transplantation.

## Materials and Methods

### *Study design*

The principal hypothesis that this study sought to examine is that the immunogenicity of donor HLA (defined as the potential of donor HLA to induce humoral alloimmunity in a specific recipient) can be predicted by assessment of their structural and physicochemical dissimilarity compared with recipient HLA molecules. To test this hypothesis, we developed a computational scoring system that enables quantitative assessment of surface electrostatic potential differences between donor and recipient HLA molecules at the tertiary structure level [three-dimensional (3D) electrostatic mismatch score (EMS-3D)]. The validity of the hypothesis was examined in a cohort of healthy females (recipient) that were sensitized to HLA through a standardized injection of donor lymphocytes from their male partner (donor). The relationship between the EMS-3D of HLA expressed on donor lymphocytes and the risk of recipient HLA-specific humoral alloimmunity (defined as detection of donor HLA-specific alloantibody using Luminex single HLA beads; this was the primary endpoint) was investigated. The study cohort comprised all women (and their male partners) who underwent their first LIT within a 2-y period (prespecified exclusion criteria are listed below).

### *LIT patient cohort*

The study cohort comprised women who had been referred to the Institute of Immunology, University Schleswig-Holstein, Campus Kiel, Germany for LIT as treatment for infertility in patients with recurrent first trimester miscarriage and/or patients with recurrent embryo implantation failure after in vitro fertilization. LIT was introduced at the Institute of Immunology, University Schleswig-Holstein, Campus Kiel, Germany in the 1980s, is approved by the local health authority, and is covered by the national health insurance providers (31, 32). LIT comprised a single intradermal injection of lymphocytes isolated from 50 ml of peripheral venous blood obtained from their male partner. The lymphocytes were separated under sterile conditions by Ficoll-Hypaque density gradient centrifugation, and after two washing steps, the cells were resuspended in 1 ml of normal saline for injection. The cellular content of the suspension was examined using phase-contrast microscopy [average cellular contents have been reported previously (32)]. The suspension, without prior storage, was given to the female partner by intradermal injection at the volar side of one forearm (32, 33). Peripheral blood was collected from all women within 2 mo before LIT and 5 wk (median: 33 d; SD: 4.5) following LIT, and serum was stored at $-21^{\circ}C$ for subsequent detection of Abs to HLA. DNA was also isolated from peripheral blood of all women and their partners for HLA typing.

This study comprised 191 consecutive women (and their male partner) who underwent their first LIT in 2009 and 2010 and had not had a previous pregnancy, blood transfusion, or organ transplantation; were not on immunosuppressive medication; and had no detectable Abs directed against their partners' HLA, as defined by complement-dependent cytotoxicity assays. During LIT, the cohort received a median (SD) of 37.4 (15.0) $\times$ $10^6$ of their partner's lymphocytes (range 20.2–83 $\times$ $10^6$ lymphocytes).

### *HLA typing*

DNA samples were genotyped using the ImmunoChip, an Illumina iSelect HD custom genotyping array, according to Illumina protocols at the Institute of Molecular Biology of Kiel University. Genotype calling was performed using Illumina GenomeStudio Data Analysis software and the custom-generated cluster file of Trynka et al. (34) based on an initial clustering of 2000 UK samples with the GenTrain 2.0 algorithm and subsequent manual readjustment and quality control. Subsequent imputation of classical HLA alleles from SNP genotypes was performed using two independent HLA imputation pipelines, HLA*IMP2 (35) and SNP2HLA (36). HLA-A and -B typing was also performed (as part of the LIT protocol) using a reverse PCR sequence-specific oligonucleotide system as implemented in the Luminex platform (LABType SSO; One Lambda, Canoga Park, CA), and the results were used for quality control in case of ambiguous results. Missing genotype data from failed genotype calls or failed quality control ($n$ = 191) were imputed, where possible, using an allele frequency-based prediction tool that considers HLA haplotype and patient race (13) ($n$ = 39 HLA class I alleles and $n$ = 92 HLA class II alleles), or excluded from further analysis ($n$ = 60 HLA class II alleles).

### *HLA-specific Ab screening*

Serum samples obtained before and after LIT were screened for HLA-specific Abs using solid-phase Luminex HLA Ab-detection beads (LABScreen; One Lambda). Selected HLA-specific Ab-positive samples were analyzed using Luminex single-Ag HLA class I and class II Ab-detection beads (One Lambda). HLA single-Ag bead-defined Ab reactivity was determined using mean fluorescence intensity (MFI) cut-off thresholds of 2000 (MFI cut-off level used clinically in our center and elsewhere to define a positive alloantibody response to a given HLA) to denote the presence of DSA and of 8000 to reflect high DSA levels (widely accepted Luminex MFI level at which DSA often results in a positive donor complement-dependent cytotoxicity crossmatch test; DSA above this level commonly denotes higher immunological risk in the context of transplantation).

### *Comparative structure modeling of HLA alleles*

Comparative structure models of all HLA class I and class II alleles represented in the HLA types of the patient cohort and of all common HLA alleles (frequency $>1\%$) were generated using the program MODELLER v9.17 (https://salilab.org/modeller/) (37). Templates for comparative structure modeling were identified by querying the Research Collaboratory for Structural Bioinformatics Protein Data Bank (PDB) using the sequence of HLA-B*07:02 and HLA-DRB1*01:01 for HLA class I and HLA class II, respectively. The search was carried out using the Domain Enhanced Lookup Time Accelerated-Basic Local Alignment Search Tool algorithm for humans (Taxonomy identification: 9606; E-value threshold of 0.005) and identified 125 HLA class I and 41 HLA class II unique crystallographically resolved structures. Of these, 12 HLA class I structures (PDB codes: 1K5N, 3MRE, 3CZF, 3BWA, 3LN4, 3SPV, 2BVP, 2A83, 3MRB, 1 $\times$ 7Q, 1OGT, 1XH3) and 22 HLA class II structures (PDB codes: 4P4R,

4P57, 4P5K, 4P5M, 1JK8, 1UVQ, 1S9V, 2NNA, 4MD4, 4MD5, 4MDJ, 3PDO, 3C5J, 1FV1, 1AQD, 1T5W, 2Q6W, 3L6F, 3QXD, 4H25, 4I5B, 4OV5) were retained for comparative modeling based on favorable indices of structural quality (Ramachandran plot, R factor, crystallographic resolution, discrete optimized protein energy, Verify3D, PROCHECK, and WHAT_CHECK scores) (38–41) and following exclusion of HLA structures resolved in complex with a ligand, such as T cell or killer Ig-related receptors (to avoid potential conformational distortion of the HLA structure occurring upon binding to the ligand). The sequences of the extracellular domain of target HLA molecules were retrieved from the European Bioinformatics Institute sequence database (ftp://ftp.ebi.ac.uk/pub/databases/ipd/imgt/hla/) and aligned using ClustalW2 using the Blocks Substitution matrix and the neighbor joining clustering algorithm and manually adjusted as indicated (42). Mean sequence homology between templates and target sequences was 91.9% (range: 84.1–100.0%). To standardize the peptide binding groove environment and eliminate structural variations between modeled molecules due to the peptide sequence, all HLA class I and class II structures were modeled with an alanine nonamer peptide and an alanine 12-mer peptide, respectively. The integrity of the modeled structures was validated using multiple objective measures of structural quality (Ramachandran plot, DOPE, Verfiy3D, PROCHECK, and WHAT_CHECK scores; data not shown).

### *Electrostatic potential calculations*

The side chains of modeled HLA structures were protonated using PROPKA (43), and atom charges and radii were assigned using the PARSE force field (44), as implemented in PDB2PQR (45), at physiological pH of 7.4. The electrostatic potential in 3D space surrounding each HLA structure was calculated numerically by solving the linearized Poisson–Boltzmann equation using the finite difference/finite element approach as implemented in the Adaptive Poisson-Boltzmann Solver (http://www.poissonboltzmann.org/) for each point on a cubic grid with sides of 353 points at a spacing of 0.33 Å. Other parameters were set as follows: ionic solution of 0.15 M of univalent positive and negative ions; protein dielectric of 2; solvent dielectric of 78; temperature of 310 K; and a probe radius of 1.4 Å (28, 46).

### *Quantitative comparison of 3D electrostatic potential between HLA molecules*

Electrostatic potential comparisons between two HLA molecules of interest were performed based on the method described by Wade et al. (47, 48) (http://pipsa.eml.org/pipsa/). As described previously (28, 49), the method considers the electrostatic potential in a region or layer of space above the molecular surface of a protein. This layer of thickness δ is defined at a distance σ from the van der Waals surface of the protein, and the electrostatic potential at the cubic grid points encompassed by this layer are considered for subsequent calculations. Electrostatic potential comparisons between two HLA molecules of interest are performed for grid points within the intersection of their layers after the two structures are superimposed (48), as shown in Fig. 1C. Quantitative comparisons are performed using the Hodgkin (50) similarity index, which assigns values between 1 (electrostatic identity, both in magnitude and sign) and −1 (electrostatic anticorrelation of the sign of the potential but of the same magnitude). These values are then converted into a distance [electrostatic similarity distance (ESD) = $\sqrt{(2-2SI)}$] to give values between 0 (electrostatic identity) and 2 (electrostatic anticorrelation) where 1 represents no apparent correlation. For the purpose of this study, a layer of δ = 4 Å thickness and raised σ = 3 Å above the molecular surface of HLA molecules was defined. These values were selected so that the electrostatic potentials compared were not highly sensitive to small changes in molecular structure (48). Electrostatic potential calculations considered the 3D space around the entire HLA molecule. Exclusion of the membrane-bound region of the HLA molecule from electrostatic potential comparisons had minimal impact on the scores (ESD) obtained (data not shown). Similarly, sampling the electrostatic potential in layers of different δ thickness (1–5 Å) and different σ distance from the molecular surface (1–5 Å) did not alter the results of the quantitative comparisons (data not shown).

For HLA alleles within a locus, electrostatic potential comparisons were made in a pairwise, all-versus-all fashion. The ESDs generated by the comparisons were compiled as a distance matrix that was then displayed as a symmetrical heat map and as a dendrogram with allele reordering such that electrostatically similar alleles cluster together. Symmetrical heat maps, dendrograms, and allele reordering were performed in R using complete-linkage hierarchical clustering as implemented in the hclust function (51).

### *EMS-3D*

The HLA type of the male partner (donor) was compared with the HLA type of the female partner (recipient) to identify mismatches in HLA-A, -B, -C, -DRB1, -DQ, and-DP loci. As shown in Fig. 1D, for HLA class I mismatches, the donor HLA was electrostatically compared with each of the recipient HLA class I alloantigens to derive the respective ESDs, and the minimum ESD value was taken to represent the EMS-3D [based on the interlocus comparison principle as previously described in our sequence-based immunogenicity algorithm (21)]. For HLA class II mismatches (Fig. 1D), the donor HLA was electrostatically compared with each of the recipient HLA within the same locus (intralocus comparison) to derive the ESDs, and the minimum value was taken to represent the EMS-3D (19).

### *Transplant patient cohort*

The patient population studied and the Ab screening protocol used have been described in detail previously (6). Briefly, the study cohort comprised 131 consecutive patients (87 males, 44 females, median age 38) who received a primary kidney allograft between 1995 and 2010 and returned to the Cambridge kidney transplant waiting list following failure of their graft during this time period (56 patients [43%] underwent transplant nephrectomy). Approximately half (50.4%) of the patients in the cohort continued to receive immunosuppression after the return to the waiting list (of those, 55% received single agent immunosuppression, and 45% received dual agent immunosuppression). Ab screening was undertaken at the time of (and prior to) the first transplant after return to the transplant waiting list following graft failure and at three monthly intervals while remaining on the list for retransplantation. Screening was undertaken using Luminex single Ag beads (One Lambda), as described above. The median (SD) duration of follow up since transplantation was 2539 (1605) d.

### *Statistics*

To investigate whether there was an association between donor HLA EMS-3D and DSA development, all HLA mismatches in the patient cohort were considered together using logistic regression models. Random effects were considered to account for potential correlations within individual patients; however, these were not found to be important and not included in the final models. An MFI ≥2000 was classified as a positive result for presence of DSA and an MFI ≥8000 was classified as a high-level DSA response. Where the donor was homozygous for a particular HLA mismatch, only one observation (mismatch) was included in the model. EMS-3D was modeled as a continuous variable and for illustration as a categorical variable by splitting into quartiles. To investigate HLA immunogenicity at an HLA locus and individual patient level, logistic regression models were used to examine the association between total EMS-3D for HLA mismatches within a locus (one or two mismatches) and development of a recipient locus-specific DSA response, adjusting for the effect of lymphocyte dose administered during LIT. Median regression models were used to model the effect of EMS-3D on post-LIT DSA MFI value. To assess nonlinearity of the explanatory variable, EMS-3D, natural cubic spline terms were added to the logistic regression model, and these terms were kept in the model if there was sufficient evidence of nonlinearity. For analyses of the transplant cohort, logistic regression models were used to investigate the relationship between donor HLA EMS-3D and DSA development at the patient level, accounting for clinical explanatory variables. Initially, each explanatory variable was modeled separately; further models investigated the additional value in incorporating EMS-3D into models, including length of time to graft failure, length of time on the waiting list after listing for retransplantation, maintenance immunosuppression regimen, graft nephrectomy, and number of administered blood transfusions. Models were compared using the log likelihood ratio statistic, and $p$ values ≤ 0.05 were considered significant. All analyses were conducted using SAS (version 9.4).

### *Study approval*

All participating couples in the LIT cohort gave informed written consent prior to inclusion in the study for use of their data and blood samples for research, and this study was approved by the local Institutional Ethics Committee (AZ D437/09, D451/12, D474/13).

### *EMS-3D software*

We are currently developing a software suite to enable HLA model building, electrostatic potential calculation, and determination of EMS-3D, which will be made freely available online (https://surgery.medschl.cam.ac.uk/divisions-and-groups/transplant-surgery/hla-structure-and-immunogenicity/immunogenicity-donor-hla-molecules/).

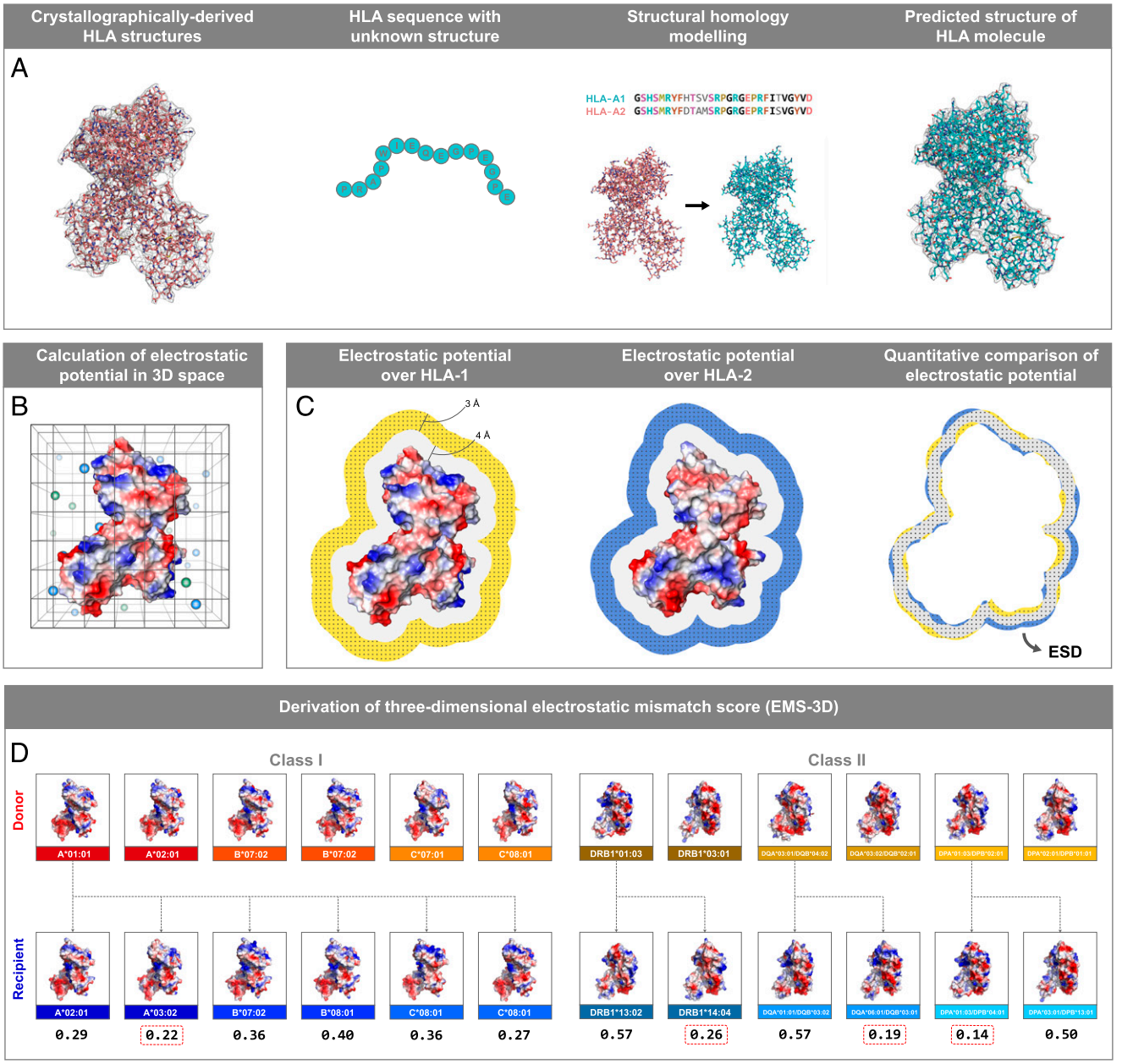


**FIGURE 1.** Schematic overview of the computational approach for quantification of surface electrostatic potential differences between HLA molecules. Bioinformatics approach to enable HLA structure prediction, surface electrostatic potential calculation, and quantification of electrostatic potential differences between two HLA molecules. (**A**) The atomic resolution structure of a given HLA class I or class II molecule is calculated using homology modeling (MODELLER) based on information derived from high-quality HLA structures resolved by x-ray crystallography. (**B**) The electrostatic potential in 3D space surrounding an HLA structure is calculated numerically by solving the linearized Poisson–Boltzmann equation for each point on a cubic grid (spacing of 0.33 Å, solvent ionic strength of 0.15 M [pH: 7.4]). (**C**) Electrostatic potential comparisons consider cubic grid points within a defined region or layer of space (of thickness $\delta = 3$Å) at a distance $\sigma$ (4 Å) above the van der Waals surface of the HLA molecule. Quantitative comparison of the electrostatic potential between two HLA molecules of interest are performed using the Hodgkin similarity index for grid points within the intersection of their layers (depicted in gray) after the two structures are superimposed, and values are converted into a distance (ESD). (**D**) Derivation of EMS-3D. A mismatched donor HLA class I molecule is compared electrostatically to each of the recipient HLA class I molecules to derive the respective ESD, and the minimum ESD value (denoted by the dashed red frame) is taken to represent the EMS-3D (interlocus comparison). Similarly, for HLA class II alloantigens, the mismatched donor HLA is compared electrostatically to each of the recipient HLA within the same locus to derive the ESDs, and the minimum value is taken to represent the EMS-3D (intralocus comparison).

## Results

*Computational approach for calculation of HLA surface electrostatic potential and quantification of differences in electrostatic potential between HLA molecules*

We generated a bioinformatics protocol to enable HLA structure prediction, surface electrostatic potential calculation, and quantification of electrostatic potential differences between different HLA molecules (Fig. 1). Because the structure of very few HLA molecules has been determined experimentally, the atomic resolution structure of a given HLA class I or class II molecule was calculated using comparative structure modeling, based on information derived from high-quality HLA structures resolved by x-ray crystallography (using the program MODELLER). Following validation of model structural quality, HLA molecules were computationally immersed

in an aqueous solvent, and the electrostatic potential in 3D space surrounding the HLA structure was calculated numerically by solving the linearized Poisson–Boltzmann equation (as implemented in the program APBS). After structure superimposition, comparisons of electrostatic potential between two HLA molecules of interest were performed in a defined region of space above the HLA molecular surface, and values were expressed as ESD, based on the Hodgkin index (as detailed in *Materials and Methods*).

The overall electrostatic potential disparity of a given donor HLA compared with recipient HLA molecules was quantified based on the EMS-3D. As described in *Materials and Methods* and shown in Fig. 1D, for HLA class I alloantigens, the mismatched donor HLA was compared electrostatically to each of the recipient HLA class I molecules to derive the respective ESDs, and the minimum ESD value was taken to represent the EMS-3D [interlocus comparison (21)]. Similarly, for HLA class II alloantigens, the mismatched donor HLA was compared electrostatically to each of the recipient HLA within the same locus to derive the ESDs, and the minimum value was taken to represent the EMS-3D [intralocus comparison (19)].

*Amino acid sequence polymorphism and disparities in surface electrostatic potential among HLA class I and class II alleles*

To investigate the relationship between amino acid sequence polymorphisms among HLA molecules and differences in their surface electrostatic potential, we performed pairwise, all-versus-all comparisons between common (frequency >1%) HLA alleles within individual HLA class I and class II loci. The ESD between HLA ranged from 0.00 to 0.777 [median: 0.307; interquartile range (IQR): 0.219–0.379], reflecting the overall structural and physicochemical similarity of molecules within the same protein family (Supplemental Table I). Overall, there was poor correlation between amino acid sequence polymorphism and electrostatic disparity for compared HLA class I ($R^2$ = 0.439) and class II molecules ($R^2$ = 0.317) with wide variation of ESD values for the same level of sequence polymorphism (Supplemental Fig. 1). It was notable that disparities in electrostatic potential were highest among HLA-DQ alloantigens and lowest among HLA-DR and -DP alloantigens, whereas HLA class I molecules had similar levels of variation in their electrostatic properties. Supplemental Fig. 2 shows the ESDs for pairs of compared HLA alleles within individual HLA loci presented as symmetrical heat maps with reordering such that electrostatically similar alleles are clustered together.

*LIT as a model of humoral alloimmunity*

Investigation of alloantibody responses against donor HLA in human transplantation is commonly confounded by many, often difficult to control, factors such as differences in allosensitization events (e.g., etiology [pregnancy, transfusion of blood products, and/or previous transplant], number, and time point), in disease context, and in immunosuppression regimens within the examined patient cohort. We overcame these limitations by studying HLA-specific alloantibody development in a unique patient cohort comprising healthy females that received a single intradermal injection of PBLs obtained from their partner as part of their treatment for infertility with LIT. The cohort comprised 191 couples with a median (SD) age of 34 (3) for females and 37 (4) for males. Comparison of male (henceforth referred to as donor) and female (henceforth referred to as recipient) HLA types revealed that the patient cohort was highly mismatched with a median number of 8 (IQR: 6–9) out of possible 12 HLA class I and class II mismatches (Fig. 2). HLA mismatches between individual donor–recipient pairs were pooled and analyzed together, accounting for

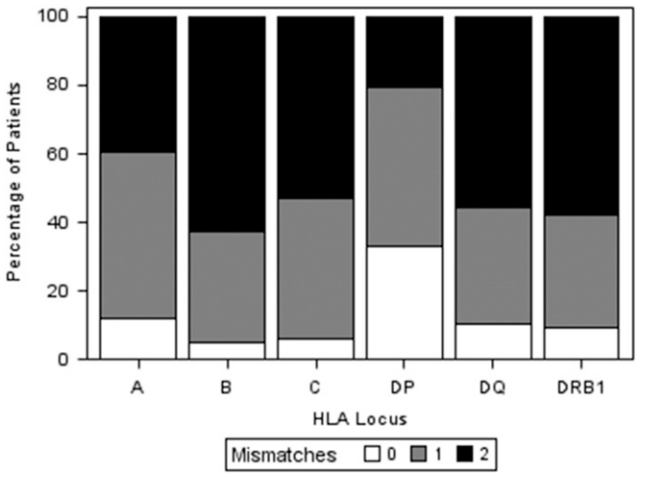


**FIGURE 2.** Distribution of HLA mismatches in the LIT patient cohort. This figure shows the percentage of patients (lymphocyte donors) with 0, 1, or 2 mismatches within HLA-A, -B, -DRB1, -DQ, and -DP loci.

potential effects at the patient level (see *Materials and Methods*). After exclusion of HLA alleles that could not be determined at two-field level (donor HLA alleles $n$ = 38; recipient HLA alleles $n$ = 22), HLA mismatches where preformed DSA was identified on pre-LIT Ab screening with Luminex solid-phase assays ($n$ = 9) and HLA mismatches that were not represented in the Luminex single-Ag bead panel ($n$ = 176), 1381 HLA mismatches were considered for further analyses (242 HLA-A, 266 HLA-B, 213 HLA-C, 257 HLA-DRB1, 247 HLA-DQ, and 156 HLA-DP).

*HLA-specific alloantibody responses after LIT*

Following LIT, HLA-specific Ab detection using Luminex showed that Ab binding against mismatched donor HLA had a median (IQR) MFI of 1039 (42, 5548). The majority of immunized recipients (84%) developed an IgG DSA response (defined as MFI ≥2000) against one or more mismatched HLA expressed on their partner's lymphocytes. Overall, DSA was detected against 569 of the 1381 (41%) donor–recipient HLA mismatches with a median (IQR) MFI of 6939 (3795, 9917). Luminex-detected binding against donor HLA-C and -DP mismatches was of low magnitude (median [SD] MFI of 40.0 [1115.0] for HLA-C and 102.4 [2868.2] for HLA-DP), and DSA responses were less frequent (DSA against 12 of 213 [6%] donor HLA-C mismatches and against 32 of 156 [21%] donor HLA-DP mismatches) compared with other loci (Fig. 3). Strong DSA responses (in frequency and magnitude) were noted against mismatches at HLA-A (160 of 242, 66%; median [IQR] MFI: 7610 [5406, 10295]), -B (138 of 266, 52%; median [IQR] MFI: 6852 [3546, 9353]), and -DQ (136 of 247, 55%; median [IQR] MFI: 7853 [4576, 11760]) loci, followed by development of DSA against donor HLA-DRB1 (91 of 257, 35%; median [IQR] MFI: 4493 [3466, 9264]) alloantigens (Fig. 3).

*Donor HLA immunogenicity and risk of development of DSA*

We examined the association between development of DSA and the immunogenicity of donor HLA mismatches as determined by comparative assessment of electrostatic potential between donor and recipient HLA (EMS-3D). Fig. 4 shows the frequency of donor–recipient HLA mismatches according to their EMS-3D grouped by HLA locus; overall, the median (IQR) EMS-3D was 0.30 (0.24–0.35) and 0.22 (0.18–0.32) for HLA class I and class II, respectively. DSA responses against HLA-C mismatches were infrequent (Supplemental Fig. 3), reflecting the relatively low expression of HLA-C on lymphocytes (52), and were therefore not

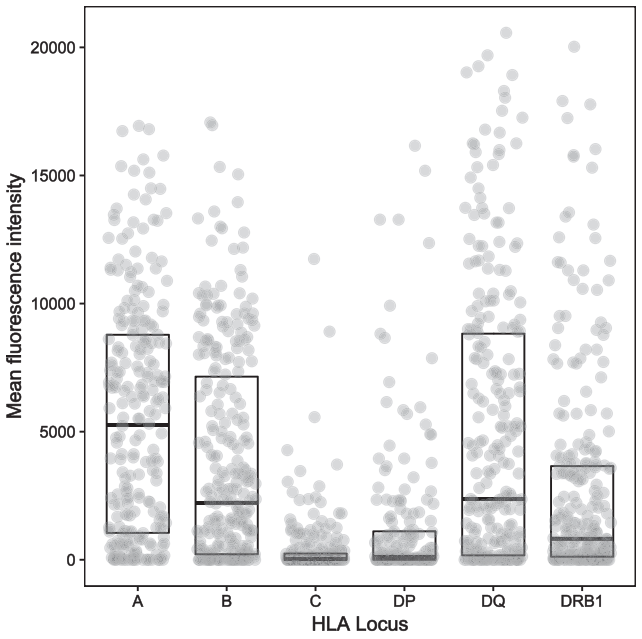


**FIGURE 3.** Donor-specific alloantibody responses after LIT against mismatched HLA expressed on donor lymphocytes. The figure depicts alloantibody binding, as detected using Luminex single HLA beads, against mismatched HLA expressed on donor lymphocytes for the entire cohort. Donor–recipient HLA mismatches ($n$ = 1381) are grouped according to HLA locus (242 HLA-A, 266 HLA-B, 213 HLA-C, 156 HLA-DP, 247 HLA-DQ, and 257 HLA-DRB1), and the MFI of DSA binding detected in recipient sera is shown on the $y$-axis. The median (SD) MFI of Ab responses against mismatches within individual HLA loci was 5270.3 (4625.6) for HLA-A, 2303.8 (4091.9) for HLA-B, 40.0 (1115.0) for HLA-C, 102.4 (2868.2) for HLA-DP, 2372.4 (5435.0) for HLA-DQ, and 803.1 (4056.2) for HLA-DRB1.

further evaluated. Logistic regression analysis showed that increasing EMS-3D of donor HLA was strongly associated with higher risk of DSA development [odds ratio (OR): 1.70 per 0.1 U increase, 95% confidence interval (CI): 1.35–2.15, $p < 0.0001$ for HLA-A and -B; OR: 2.56 per 0.1 U increase, 95% CI: 2.13, 3.07, $p < 0.0001$ for HLA-DRB1, -DQ, and -DP (Table I)]. HLA-DP was the least immunogenic locus (excluding HLA-C), and it was notable that differences in electrostatic potential among HLA-DP mismatches were of lower magnitude compared with other loci (EMS-3D median: 0.19; IQR: 0.18–0.24). The observed low immunogenicity of donor HLA-DP, however, might in part reflect a lower cell surface expression of HLA-DP on lymphocytes compared with -DR and -DQ molecules (53–56). In contrast, physicochemical differences between donor and recipient HLA-DQ were higher compared with other loci (EMS-3D median: 0.35; IQR: 0.20–0.42), and donor HLA-DQ with the highest EMS-3D (within the fourth compared with first quartile) were highly likely to induce a DSA response (OR: 27.7, 95% CI: 10.4–73.9; $p < 0.0001$). HLA-DRB1 mismatches had lower EMS-3D scores (EMS-3D median: 0.20; IQR: 0.17–0.24) and were less immunogenic compared with HLA-DQ, similar to what has been reported on the relative frequency of HLA-DRB1 and -DQ DSA responses after renal transplantation (14).

### *Relationship between donor HLA EMS-3D and probability of humoral alloresponse*

The potential of this approach to predict the immunogenic potential of donor HLA was examined further by considering the probability of an alloantibody response after LIT according to the EMS-3D of donor HLA alloantigens, using logistic regression modeling. As shown in Fig. 5, this analysis demonstrated a strong relationship between donor–recipient HLA electrostatic disparity and predicted probability of an alloantibody response for all loci examined. Wider CIs were observed for the immunogenic potential of high EMS-3D HLA-DR and -DP alloantigens, and this reflected the relatively low number of observations for such mismatches in the patient cohort. The association was strongest for HLA-DQ alloantigens (Fig. 5D), and it is notable that multiple recent studies have highlighted the predominance of HLA-DQ–specific humoral alloresponses after solid organ transplantation (57–60). Overall, our model predicts that donor HLA class I and class II (HLA-A, -B, -DRB1, -DQ, and -DP) with low EMS-3D have an ~10% probability of inducing DSA (e.g., the observed probability of an alloantibody response for HLA with EMS-3D <0.045 was 11% [of 27 mismatched HLA-3–induced DSA]). This probability increases to over 75% for donor HLA with the highest EMS-3D (e.g., the observed probability of a DSA response for donor HLA with EMS-3D >0.38 was 71% [of 110 mismatched HLA-78–induced DSA]). Fitting the model to examine high-level DSA responses (defined as DSA MFI ≥8000, which, in the context of transplantation, commonly denotes high immunological risk) showed a near linear association between donor HLA EMS-3D and predicted probability of DSA development (Fig. 5G).

### *Relationship between donor HLA EMS-3D and DSA MFI level after LIT*

We next considered the relationship between donor HLA EMS-3D and the magnitude of the alloantibody response as assessed based on the MFI binding detected in the Luminex assay. The latter provides semiquantitative information on the level of circulating alloantibody, and previous studies have shown an association between DSA MFI level and clinical outcome (5, 61, 62). Median regression analysis showed that donor HLA with increasing EMS-3D were associated with progressively stronger (higher MFI) alloantibody responses following LIT ($p < 0.001$; Fig. 6). The magnitude of the alloantibody response increased from a median MFI of 48 (IQR: 0–300) for donor HLA class I and II (HLA-A, -B, -DRB1, and -DQ) with EMS-3D <0.14 to a median MFI of 6432 (IQR: 1,876–10,002) for alloantigens with EMS-3D >0.35 (Fig. 6). The association between donor HLA EMS-3D and MFI binding level was strongest for donor HLA class II mismatches (Fig. 6B).

Donor homozygosity for a given HLA class I or II mismatch had no effect on the risk of DSA development (data not shown). Although there was evidence that alloantibody responses were more likely the higher the amount of donor lymphocytes administered during LIT (adjusted OR: 1.02 per $10^6$ increase in lymphocyte dose, 95% CI: 1.01–1.03; $p < 0.0001$), adjusting for donor lymphocyte dose did not alter the relationship between donor HLA EMS-3D and risk of DSA development. In the analyses above, donor–recipient HLA mismatches and their immunogenic potential were considered individually and independently from each other. To consider HLA immunogenicity at a locus and individual patient level, we examined the association between the overall immunogenic potential of HLA mismatches within a locus (as assessed by EMS-3D) and the likelihood of a recipient locus-specific DSA response [as suggested by other authors (14, 63)]. This analysis showed that locus-specific EMS-3D was strongly associated with HLA-A, -B, -DRB1, -DQ, and -DP DSA development (OR: 1.40 per 0.1 U increase; 95% CI: 1.21–1.61, $p < 0.0001$ for HLA-A and -B; OR: 1.57 per 0.1 U increase; 95% CI: 1.40–1.77, $p < 0.0001$ for HLA-DR, -DQ, and -DP) independent of lymphocyte dose administered during LIT.

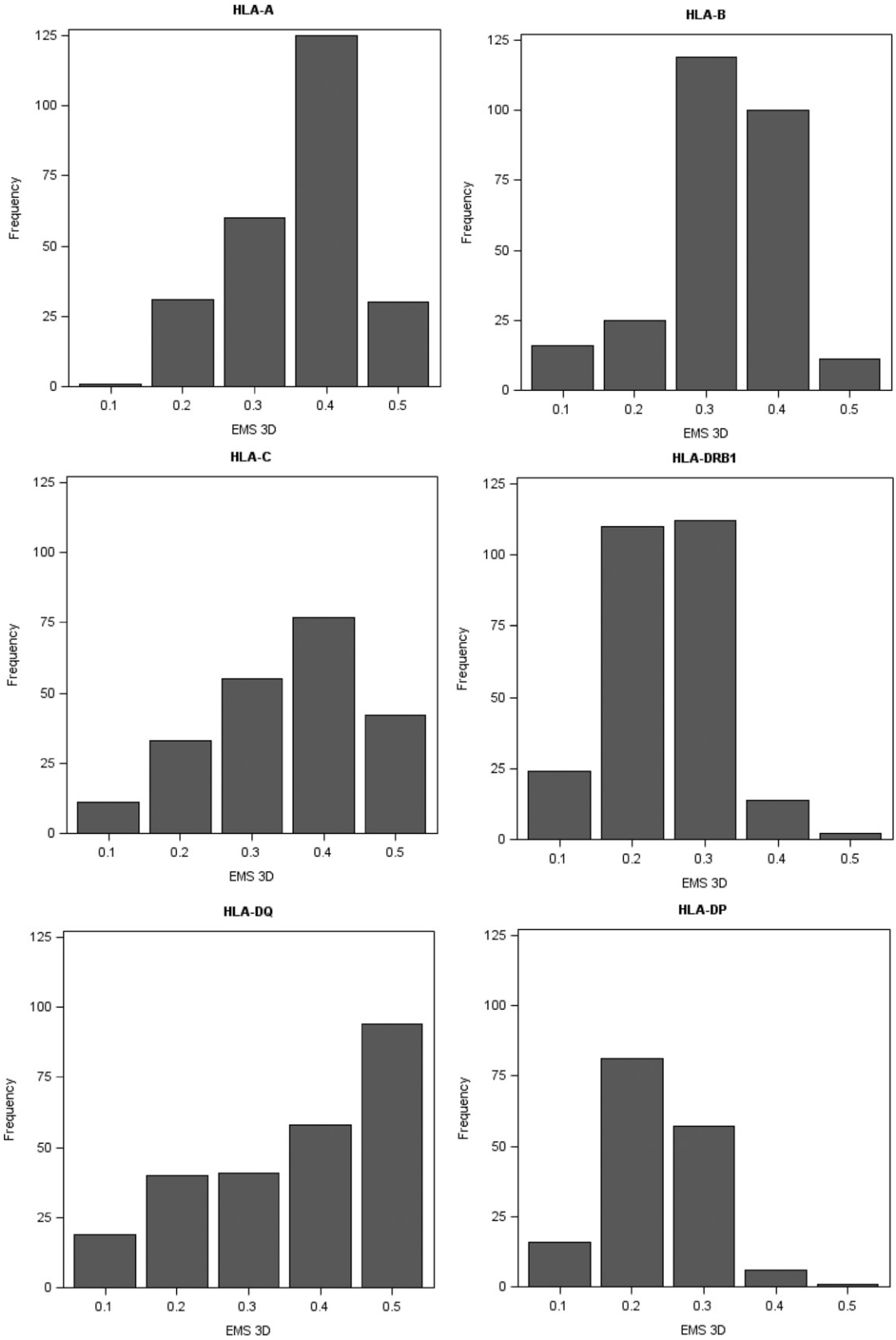


**FIGURE 4.** Frequency of HLA class I and class II mismatches in the LIT patient cohort according to their EMS-3D. The figure depicts the frequency of donor–recipient HLA mismatches according to their EMS-3D, grouped by HLA locus. The median (IQR) EMS-3D for individual loci was HLA-A: 0.32 (0.27–0.36); HLA-B: 0.28 (0.22–0.33); HLA-C: 0.32 (0.22–0.40); HLA-DRB1: 0.20 (0.17–0.24); HLA-DQ: 0.35 (0.20–0.42); and HLA-DP: 0.19 (0.18–0.24).

Table I. Influence of donor HLA immunogenicity, as assessed by EMS-3D, and risk of development of donor-specific alloantibody after LIT

| | | OR on Developing HLA DSA (MFI ≥ 2000) | |
|---|---|---|---|
| *HLA* Locus | Donor HLA MM, DSA | OR (95% CI) | *p* Value |
| *HLA-A* | *n* = 242, 160 events | | |
| EMS-3D | | 1.64 (1.14, 2.37) | 0.007 |
| *HLA-B* | *n* = 266, 138 events | | |
| EMS-3D | | 1.57 (1.15, 2.15) | 0.004 |
| *HLA-DRB1* | *n* = 257, 91 events | | |
| EMS-3D | | | < 0.0001 |
| *HLA-DQ* | *n* = 247, 136 events | | |
| EMS-3D | | 2.64 (2.01, 3.48) | < 0.0001 |
| *HLA-DP* | *n* = 156, 32 events | | |
| EMS-3D | | 3.32 (1.41, 7.81) | 0.004 |
| *HLA-A+B* | *n* = 508, 298 events | | |
| EMS3D | | 1.70 (1.35, 2.15) | < 0.0001 |
| *HLA-DP+DQ+DRB1* | *n* = 660, 259 events | | |
| EMS3D | | 2.56 (2.13, 3.07) | < 0.0001 |
| *HLA-A+B+DP+DQ+DRB1* | *n* = 1168, 557 events | | |
| EMS3D | | 2.35 (2.04, 2.71) | < 0.0001 |

Logistic regression models were used to investigate the association between donor HLA EMS-3D and donor-specific alloantibody development. ORs are omitted where natural cubic splines were fitted.

MM, mismatches.

### *Analysis of HLA-specific Ab responses after kidney transplantation*

We next considered, in a proof of principle study, the applicability of our approach in the kidney transplantation setting. Alloantibody responses against donor HLA expressed on renal allografts were examined in a cohort of 131 kidney transplant recipients returning to the transplant waiting list following first graft failure. Humoral responses against HLA class II alloantigens predominate long term after kidney transplantation and are strongly associated with graft failure (1), and, therefore, this analysis focused on development of DSA against mismatched HLA class II alloantigens. The demographic and transplant characteristics of the patient cohort have been published previously (6). To account for factors that may influence HLA-specific Ab responses at an individual patient level, multivariable logistic regression analysis of the association between EMS-3D of donor kidney HLA-DRB1 and -DQ mismatches and DSA development was adjusted for length of time to graft failure, length of time on the waiting list after listing for retransplantation, maintenance immunosuppression regimen while on the transplant waiting list, graft nephrectomy, and number of administered blood transfusions. Similar to the findings on DSA responses after LIT, this analysis showed that the EMS-3D of HLA-DRB1 and -DQ mismatches expressed on donor kidneys were independently correlated with the risk of development of DSA after kidney transplant failure (OR: 1.86 per 0.1 U increase in EMS-3D, 95% CI: 1.07–3.23, $p = 0.028$ for HLA-DRB1; OR: 1.90 per 0.1 U increase in EMS-3D, 95% CI: 1.25–2.88, $p = 0.0026$ for HLA-DQ).

## Discussion

The capacity of donor HLA to stimulate alloantibody responses (HLA immunogenicity) is dependent upon their structural recognition by receptors on recipient B cells that initiate the immune response, and previous work has suggested that HLA immunogenicity should be considered in the context of amino acid sequence polymorphisms between donor and recipient HLA molecules (12, 21, 64). The present investigation introduces a fundamentally new approach at evaluating the immunogenic potential of donor HLA focusing entirely on their tertiary structure and on their unique structural and surface electrostatic potential properties compared with recipient HLA molecules. We have developed a computational approach to compare and quantify HLA electrostatic properties at atomic resolution level and applied it to predict HLA-specific alloantibody development in a unique model of human sensitization. We show that 1) HLA molecules differ widely at the level of electrostatic potential in 3D space, and these differences are not explicable on account of the underlying amino acid sequence polymorphisms; 2) the electrostatic disparity of a donor HLA compared with recipient HLA molecules, as assessed by EMS-3D, was strongly associated with the risk of development of donor-specific alloantibody; and 3) electrostatic potential disparities are highest among HLA-DQ molecules, which were the most immunogenic alloantigens in this study and whose immunogenicity conformed best to our EMS-3D algorithm. Taken together with our proof of principle study in the setting of human kidney transplantation, the present investigation provides, to our knowledge, important first validation that donor HLA immunogenicity can be predicted based on assessment of their unique surface electrostatic potential properties compared with recipient HLA molecules.

The risk of allosensitization after transplantation increases incrementally with the number of HLA mismatches at individual HLA class I and class II loci (6). However, simple enumeration of differences at the whole Ag level is constrained by limited possible values (zero, one, or two mismatches per locus) and does not account for differences in donor HLA immunogenicity for a given recipient. Current approaches for determining the potential of a donor HLA to induce an alloantibody response are based on quantifying the degree of dissimilarity between the donor and recipient HLA molecules (12, 17, 19, 21, 65). The most frequently used methods (HLAMatchmaker and Cambridge HLA immunogenicity algorithm) evaluate differences in the number and location of amino acid mismatches at continuous and discontinuous (eplets) positions on the HLA sequence, and multiple studies have suggested they provide superior risk stratification over conventional HLA mismatch grade for predicting development of DSA, allograft rejection, transplant glomerulopathy, and allograft survival (14, 16, 18, 20, 63). Both of these methods reflect differences in amino acid sequence between donor and recipient HLA mismatches and generate highly correlated scores that provide a similar assessment of HLA immunogenicity (18, 66). Importantly, accounting for the physicochemical properties of donor HLA amino acid polymorphisms appears to improve prediction of DSA development against HLA class I alloantigens (18, 19).

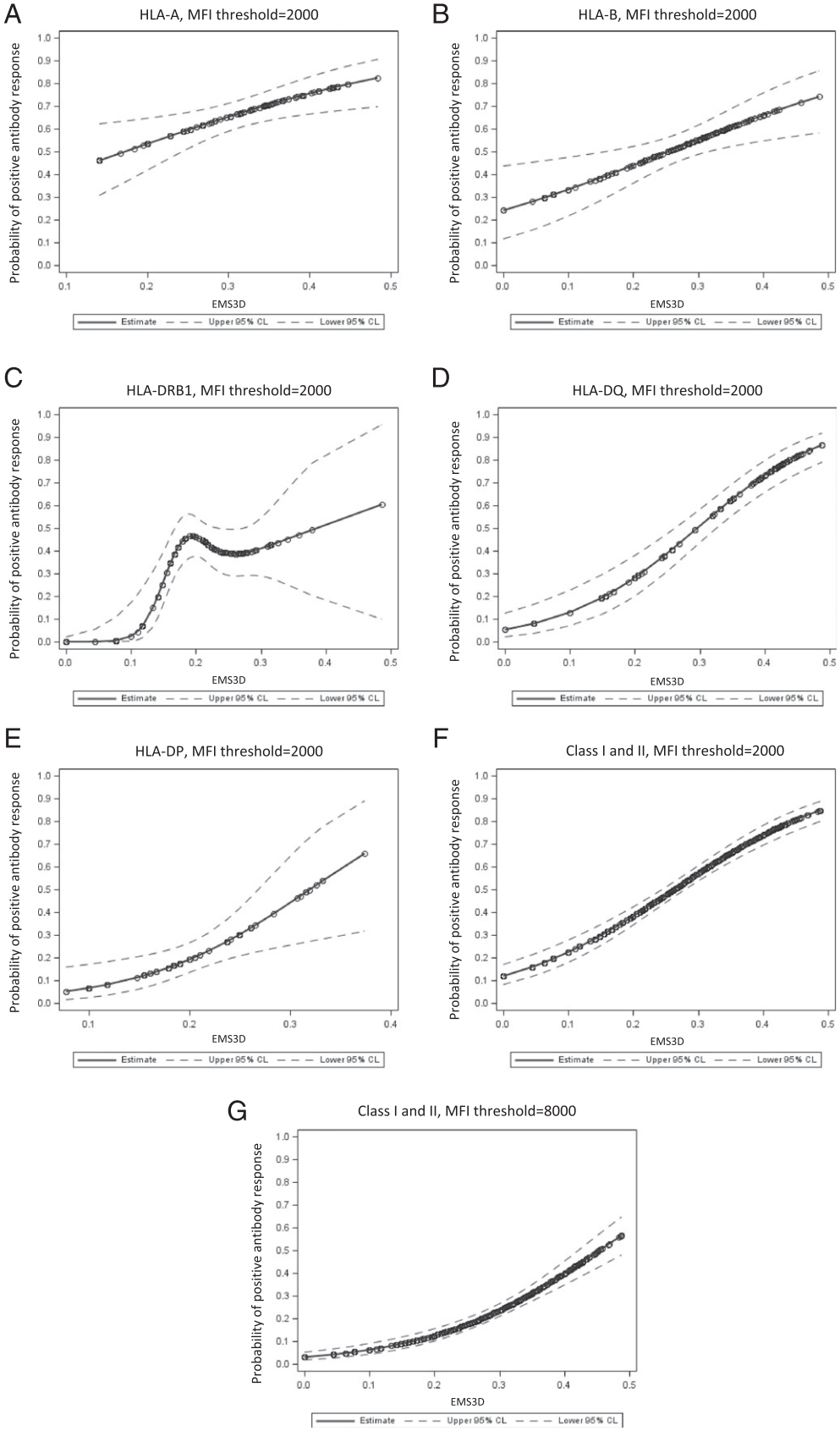


**FIGURE 5.** Probability of donor-specific alloantibody response after LIT according to the EMS-3D of mismatched HLA on donor lymphocytes. The relationship between the immunogenic potential of donor HLA, as determined by EMS-3D, and the probability of a donor-specific alloantibody response after LIT was examined using logistic regression modeling. Each panel shows a logistic regression model with 95% CI (dotted lines) for individual HLA loci (**A**–**E**) and for HLA class I and class II loci combined (**F** and **G**). DSA responses against HLA-C mismatches were infrequent and were not examined. Donor-specific alloantibody responses were defined using MFI cut-off thresholds ≥2000 (A–F) and ≥8000 (G). Wide CIs for alloantibody responses against HLA-DR and -DP alloantigens reflect the relatively low number of observations for HLA-DR and -DP mismatches with high EMS-3D scores in the LIT patient cohort. Relatively few alloantibody responses with MFI ≥8000 were noted against HLA-DP alloantigens ($n$ = 7), and, therefore, HLA-DP mismatches were not included in the (G) model.

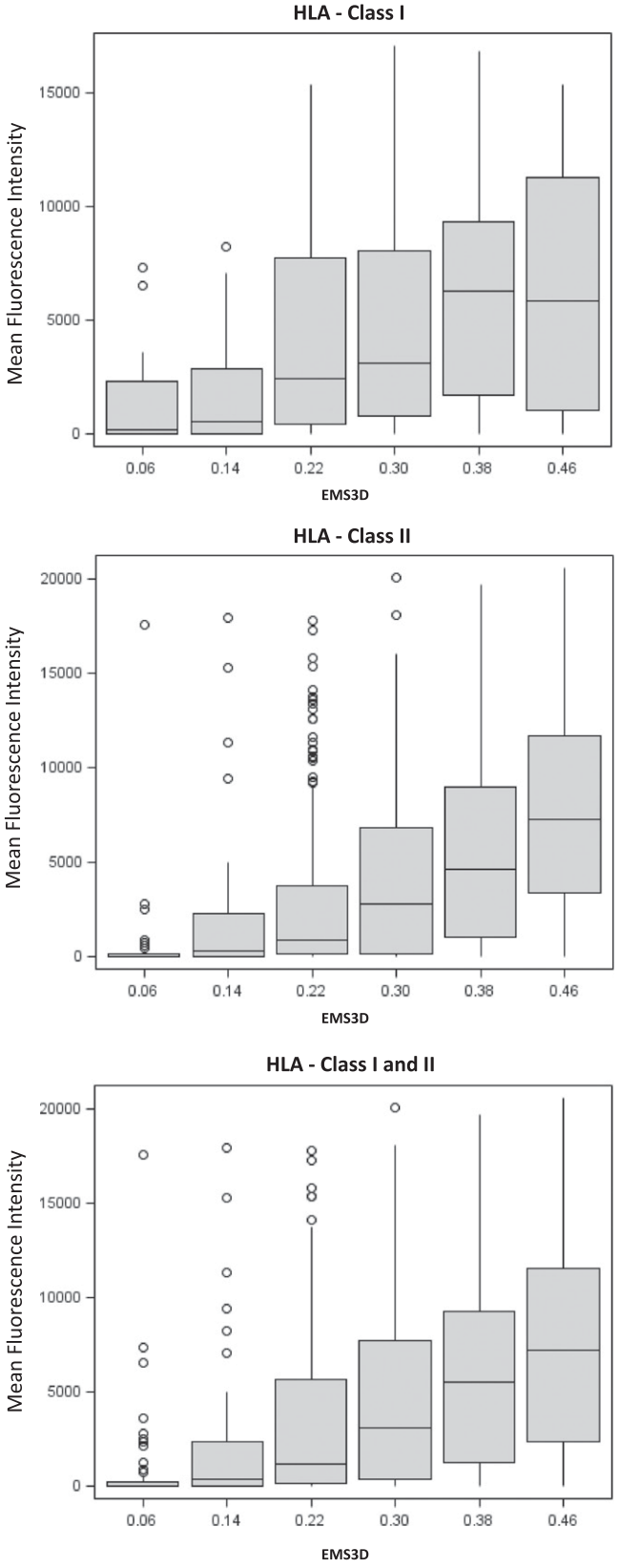


**FIGURE 6.** Relationship between donor HLA EMS-3D and the donor-specific MFI binding level of alloantibodies developed after LIT. The relationship between EMS-3D of mismatched HLA on donor lymphocytes and the magnitude of DSA binding, as assessed based on MFI, detected in the Luminex single Ag bead assay, is depicted. Donor HLA mismatches are grouped according to EMS-3D and the box plots depict the median MFI (horizontal blue line) and IQR (box) of MFI values (the lines show maximum MFI values) for DSA binding within each group. Median regression analysis showed that donor HLA with increasing EMS-3D were associated with progressively stronger (higher MFI) alloantibody responses following LIT ($p < 0.001$). Alloantibody responses against donor HLA-C and -DP mismatches were infrequent and of low MFI value and are, therefore, not included in this analysis.

Protein electrostatics reflect the amino acid composition of their primary structure but are mainly determined by the number and distribution of polar and charged residues, the protonation state of ionizable groups within a given ionic environment, and their ability to form specific bonding interactions, such as salt bridges and hydrogen bonds. Importantly, our study shows that the variation in surface electrostatic potential between HLA molecules cannot be inferred on account of differences at the amino acid sequence level, and relatively poor correlation exists between residue polymorphisms and electrostatic disparity among HLA class I and class II molecules (Supplemental Fig. 1). Given that hydrophobic patches on a protein surface tend to have low electrostatic potential compared with an acidic, basic or polar patch, the electrostatic potential also captures aspects of the protein's hydrophobic interaction properties. Electrostatic forces are important determinants of the affinity and specificity of macromolecular interactions, and it has been suggested that the process of affinity maturation involves optimization of electrostatic interactions in the BCR–Ag binding site (24, 25, 67, 68). Our study showed that donor HLA with high versus low EMS-3D were more likely to induce a specific alloantibody response, and, therefore, it would be tempting to speculate that alloantigens with disparate electrostatic potential profiles compared with recipient HLA molecules lead to more efficient BCR recognition in the secondary lymphoid organs and to improved selection and survival of differentiated B cells during the process of affinity maturation in the germinal center. Indeed, recent insights into the mechanisms that determine the fate decision of proliferating, Ag-activated B cells at the pregerminal center stage suggested that B cells with higher affinity to their Ag presented more HLA peptide to and made longer-lasting contact with cognate T follicular helper cells at the B cell–T cell border in secondary lymphoid organs, resulting in more T cell help and differentiation into germinal center B cells (with further BCR diversification through somatic hypermutation) (69, 70). In contrast, proliferating B cells with lower affinity to their Ag may form less durable T follicular helper cell–B cell conjugates and are more likely to develop into germinal center–independent memory B cells (that undergo class switching but not somatic hypermutation) (71). The implication of this model of Ag-activated B cell differentiation for the present investigation is that alloantibody responses to donor HLA with high EMS-3D might be derived by germinal center–dependent B cells and are of high affinity, whereas humoral responses to donor HLA with lower EMS-3D, when triggered, might be derived by germinal center–independent B cells and are more broadly reactive and of lower affinity. It would be interesting to investigate this hypothesis in future studies.

Multiple studies over recent years have provided strong evidence in support of the association between the development of donor HLA-specific alloantibodies and the risk of acute Ab-mediated rejection, chronic rejection, and allograft loss across all solid organ transplants (63, 72–77). The ability to assess the risk of posttransplant humoral alloimmunity associated with particular donor–recipient HLA combinations is of major clinical interest, both to inform organ allocation policies and to enable more efficient immune monitoring and individualization of immunosuppression protocols to help prevent de novo DSA development.

The present study suggests that the probability of an alloantibody response (generation and magnitude) against a donor HLA-A, -B, -DRB1, -DQ, or -DP alloantigen increases with increasing EMS-3D. Although our study does not enable identification of an HLA immunogenicity threshold in the setting of clinical transplantation, our findings suggest that it might be possible to identify a substantial number of low EMS-3D HLA mismatches that might be tolerated by the immune system of a given recipient. DSA development against both HLA class I and class II alloantigens increases the risk of subsequent rejection and allograft failure, but humoral responses against HLA class II seem to predominate, and these most commonly involve HLA-DQ–specific alloantibodies (58–60, 78). Our analysis of the most common HLA-DQ alleles (Supplemental Fig. 1) showed that electrostatic potential disparities are highest among HLA-DQ alloantigens (with only a modest correlation between ESD and the underlying amino acid sequence polymorphism) compared with other loci, and this may account for their increased immunogenic potential. Notably, HLA-DQ immunogenicity conformed best to our prediction model with a strong association between donor EMS-3D and probability of a DSA response in the LIT cohort, whereas a strong association between HLA-DQ EMS-3D and DSA development was also noted in the kidney transplant cohort.

The present study has focused on the structural aspects of donor HLA allorecognition that influence the subsequent humoral response by recipient B cells. Our computational protocol enables quantification of electrostatic potential differences between donor and recipient HLA, accounting for the entire 3D space around the HLA molecule to produce an average score. Exclusion of the membrane-bound area of the HLA did not alter the results of our analysis as this part of the molecule is relatively monomorphic and therefore similar among different HLA. However, it is possible that a small surface area on a donor HLA that differs widely in electrostatic potential from the respective area on recipient HLA might be sufficient to drive the alloimmune response, although the average difference across the entire molecule remains low. Our computational method can be adapted to incorporate immunogenic "hot-spots" on the HLA molecular surface (e.g., functional B cell epitopes), and this is the subject of our current research (28). It is also important to recognize that proliferation and differentiation of Ag-specific naive B cells into memory B cells and long-lived plasma cells requires T cell help through linked recognition of Ag-derived peptides presented in the context of B cell HLA class II molecules. Previous observational studies highlighted the importance of the HLA-DR phenotype of the recipient in humoral alloresponses to donor HLA class I alloantigens (79, 80), and, more recently, this concept has been extended to evaluate the capacity of recipient HLA-DR molecules to bind donor HLA class I– and class II–derived peptides using the NetMHCIIpan computational method and to examine the contribution of this pathway to DSA development (81–84). Computational prediction of HLA class II–restricted epitopes by $CD4^+$ T cells is of great interest for understanding immune responses in the context of transplantation, autoimmunity, infection, and cancer, but it is a difficult and complex undertaking because of the open conformation of the HLA class II peptide binding groove that can accommodate peptides of variable length (10–30 aa long) and because of the fact that Ag processing and peptide loading are incompletely understood (85). Nevertheless, this is the subject of intense research, and a multitude of computational methods are currently available for predicting HLA class II peptide binding, with mixed results (86, 87). Despite the strong association between the surface electrostatic potential properties of donor HLA and alloantibody responses in the current study, DSA development was noted against HLA with low EMS-3D and vice versa. Consideration of HLA class II peptide presentation to $CD4^+$ T cells is likely to improve the predictive ability of our immunogenicity algorithm, and we are currently undertaking relevant studies to explore this question. To this extent, it would be intriguing to examine the contribution of electrostatic interactions within the pockets of the HLA class II peptide binding groove to high-affinity peptide binding (49, 88).

A strength of the current study is that HLA immunogenicity was investigated in a unique model of HLA sensitization comprising nonsensitized individuals that underwent a single sensitizing event (injection of donor lymphocytes), followed by detection of HLA-specific development approximately 5 wk later. To our knowledge, this is the first study to systematically examine HLA immunogenicity in this setting, thus avoiding commonly encountered confounders in similar studies, including variations in baseline disease, nonuniform immunosuppression protocols, and unknown and variable sensitization events (previous transplants, pregnancies, and blood transfusions). We acknowledge that it would have been interesting to examine the temporal evolution of the immune response at different time points, but this was not possible as further serum samples were not routinely collected. The kinetics of IgG HLA-specific Ab development after exposure to human lymphocytes have not been studied in detail, especially using sensitive detection methods, but it is well documented that specific humoral responses (class switched and affinity matured) peak within 30 d from exposure to Ag (71), and a previous study in the context of LIT suggested that the alloresponse peaks during the second month after lymphocyte immunization (89). It is, therefore, unlikely that relevant alloantibody responses have been missed because of the timing of serum collection in this study. Another limitation of the study is that a relatively small cohort of patients was examined to investigate development of DSA after failure of kidney transplant, and our findings would be strengthened if they were confirmed in larger cohorts and in patients with functioning grafts that are prospectively monitored for alloantibody development, accounting for immunosuppression regimen, drug levels, and for noncompliance. Similarly, our study was not powered to compare the predictive ability of our structural HLA immunogenicity algorithm relative to currently available, amino acid sequence–based methods, and, therefore, future studies are warranted to address this limitation and help identify the best approach, or combination of methods, to improve immunological risk assessment in the clinical transplantation setting. We were unable to systematically assess the immunogenicity of HLA-C and -DP alloantigens because of their relatively low expression on lymphocytes. Alloantibodies against HLA-DP can cause humoral rejection after kidney transplantation, and mismatching at the -DP locus is associated with decreased graft survival in patients undergoing repeat kidney transplantation (90, 91). Within the confines of the lymphocyte HLA sensitization model, HLA-DP immunogenicity seemed to conform to our algorithm, and it would be interesting to examine the applicability of our approach in the transplant setting, both in terms of predicting HLA-DP–specific sensitization and for analysis of the relevant effect of -DP mismatching on renal transplant outcomes. Finally, this study focused on DSA detection based on the Luminex solid phase assay. It would be interesting to examine a more functional readout of the humoral response, such as the ability of DSA to cause complement-dependent cell lysis. However, the latter would require access to very large panels of lymphocytes with appropriately selected HLA types and would need careful interpretation of the results (e.g., levels of HLA expression among different lymphocyte panels, potential cross-reactivity with multiple HLA targets expressed on lymphocytes, etc.). Alternatively, the Luminex C1q assay has been used to detect complement-binding alloantibodies. We, and others, have

questioned the clinical value of the Luminex C1q assay readout and showed that C1q binding in the Luminex assay is closely related to Ab MFI level (92–94). Accordingly, based on our finding that donor HLA EMS-3D correlated strongly with DSA defined at MFI >8000, we would anticipate a similarly strong relationship between EMS-3D and C1q binding DSA. Such an analysis, however, was beyond the scope of our study.

In conclusion, the present investigation demonstrates a clear relationship between the electrostatic properties of HLA molecules and their immunogenic potential. Quantification of electrostatic potential differences at the tertiary level between donor and recipient HLA molecules enables prediction of humoral alloimmune responses in the context of lymphocyte allosensitization. We have shown the translational potential of this approach in the clinical setting of kidney transplantation. Our approach has the potential to identify acceptable HLA mismatches for a given recipient, thereby increasing access to suitable donors that are currently considered a poor match, to enable better immunological risk assessment, and to decrease the burden of allosensitization and humoral rejection after solid organ transplantation.

## Disclosures

The authors have no financial conflicts of interest.

## References


1. Wiebe, C., I. W. Gibson, T. D. Blydt-Hansen, D. Pochinco, P. E. Birk, J. Ho, M. Karpinski, A. Goldberg, L. Storsley, D. N. Rush, and P. W. Nickerson. 2015. Rates and determinants of progression to graft failure in kidney allograft recipients with de novo donor-specific antibody. *Am. J. Transplant.* 15: 2921–2930.
2. Mehra, N. K., J. Siddiqui, A. Baranwal, S. Goswami, and G. Kaur. 2013. Clinical relevance of antibody development in renal transplantation. *Ann. N. Y. Acad. Sci.* 1283: 30–42.
3. Lefaucheur, C., A. Loupy, D. Vernerey, J. P. Duong-Van-Huyen, C. Suberbielle, D. Anglicheau, J. Vérine, T. Beuscart, D. Nochy, P. Bruneval, et al. 2013. Antibody-mediated vascular rejection of kidney allografts: a population-based study. *Lancet* 381: 313–319.
4. Tible, M., A. Loupy, D. Vernerey, C. Suberbielle, T. Beuscart, A. Cazes, R. Guillemain, C. Amrein, V. Pezzella, J. N. Fabiani, et al. 2013. Pathologic classification of antibody-mediated rejection correlates with donor-specific antibodies and endothelial cell activation. *J. Heart Lung Transplant.* 32: 769–776.
5. Lefaucheur, C., A. Loupy, G. S. Hill, J. Andrade, D. Nochy, C. Antoine, C. Gautreau, D. Charron, D. Glotz, and C. Suberbielle-Boissel. 2010. Preexisting donor-specific HLA antibodies predict outcome in kidney transplantation. *J. Am. Soc. Nephrol.* 21: 1398–1406.
6. Kosmoliaptsis, V., O. Gjorgjimajkoska, L. D. Sharples, A. N. Chaudhry, N. Chatzizacharias, S. Peacock, N. Torpey, E. M. Bolton, C. J. Taylor, and J. A. Bradley. 2014. Impact of donor mismatches at individual HLA-A, -B, -C, -DR, and -DQ loci on the development of HLA-specific antibodies in patients listed for repeat renal transplantation. *Kidney Int.* 86: 1039–1048.
7. Meier-Kriesche, H. U., J. C. Scornik, B. Susskind, S. Rehman, and J. D. Schold. 2009. A lifetime versus a graft life approach redefines the importance of HLA matching in kidney transplant patients. *Transplantation* 88: 23–29.
8. Opelz, G., and B. Döhler. 2012. Association of HLA mismatch with death with a functioning graft after kidney transplantation: a collaborative transplant study report. *Am. J. Transplant.* 12: 3031–3038.
9. Zachary, A. A., and M. S. Leffell. 2016. HLA mismatching strategies for solid organ transplantation - a balancing act. *Front. Immunol.* 7: 575.
10. Doxiadis, I. I., J. M. Smits, G. M. Schreuder, G. G. Persijn, H. C. van Houwelingen, J. J. van Rood, and F. H. Claas. 1996. Association between specific HLA combinations and probability of kidney allograft loss: the taboo concept. *Lancet* 348: 850–853.
11. Gracie, J. A., E. M. Bolton, C. Porteous, and J. A. Bradley. 1990. T cell requirements for the rejection of renal allografts bearing an isolated class I MHC disparity. *J. Exp. Med.* 172: 1547–1557.
12. Duquesnoy, R. J. 2006. A structurally based approach to determine HLA compatibility at the humoral immune level. *Hum. Immunol.* 67: 847–862.
13. Duquesnoy, R. J. 2002. HLAMatchmaker: a molecularly based algorithm for histocompatibility determination. I. Description of the algorithm. *Hum. Immunol.* 63: 339–352.
14. Wiebe, C., D. Pochinco, T. D. Blydt-Hansen, J. Ho, P. E. Birk, M. Karpinski, A. Goldberg, L. J. Storsley, I. W. Gibson, D. N. Rush, and P. W. Nickerson. 2013. Class II HLA epitope matching-A strategy to minimize de novo donor-specific antibody development and improve outcomes. *Am. J. Transplant.* 13: 3114–3122.
15. Kosmoliaptsis, V., J. A. Bradley, L. D. Sharples, A. Chaudhry, T. Key, R. S. Goodman, and C. J. Taylor. 2008. Predicting the immunogenicity of human leukocyte antigen class I alloantigens using structural epitope analysis determined by HLAMatchmaker. *Transplantation* 85: 1817–1825.
16. Sapir-Pichhadze, R., K. Tinckam, K. Quach, A. G. Logan, A. Laupacis, R. John, J. Beyene, and S. J. Kim. 2015. HLA-DR and -DQ eplet mismatches and transplant glomerulopathy: a nested case-control study. *Am. J. Transplant.* 15: 137–148.
17. Duquesnoy, R. J. 2017. Are we ready for epitope-based HLA matching in clinical organ transplantation? *Transplantation* 101: 1755–1765.
18. Kosmoliaptsis, V., D. H. Mallon, Y. Chen, E. M. Bolton, J. A. Bradley, and C. J. Taylor. 2016. Alloantibody responses after renal transplant failure can be better predicted by donor-recipient HLA amino acid sequence and physicochemical disparities than conventional HLA matching. *Am. J. Transplant.* 16: 2139–2147.
19. Kosmoliaptsis, V., L. D. Sharples, A. N. Chaudhry, D. J. Halsall, J. A. Bradley, and C. J. Taylor. 2011. Predicting HLA class II alloantigen immunogenicity from the number and physiochemical properties of amino acid polymorphisms. *Transplantation* 91: 183–190.
20. Kosmoliaptsis, V., L. D. Sharples, A. Chaudhry, R. J. Johnson, S. V. Fuggle, D. J. Halsall, J. A. Bradley, and C. J. Taylor. 2010. HLA class I amino acid sequence-based matching after interlocus subtraction and long-term outcome after deceased donor kidney transplantation. *Hum. Immunol.* 71: 851–856.
21. Kosmoliaptsis, V., A. N. Chaudhry, L. D. Sharples, D. J. Halsall, T. R. Dafforn, J. A. Bradley, and C. J. Taylor. 2009. Predicting HLA class I alloantigen immunogenicity from the number and physiochemical properties of amino acid polymorphisms. *Transplantation* 88: 791–798.
22. Hopp, T. P., and K. R. Woods. 1981. Prediction of protein antigenic determinants from amino acid sequences. *Proc. Natl. Acad. Sci. USA* 78: 3824–3828.
23. Potocnakova, L., M. Bhide, and L. B. Pulzova. 2016. An introduction to B-cell epitope mapping and in silico epitope prediction. *J. Immunol. Res.* 2016: 6760830.
24. Chong, L. T., Y. Duan, L. Wang, I. Massova, and P. A. Kollman. 1999. Molecular dynamics and free-energy calculations applied to affinity maturation in antibody 48G7. *Proc. Natl. Acad. Sci. USA* 96: 14330–14335.
25. Lippow, S. M., K. D. Wittrup, and B. Tidor. 2007. Computational design of antibody-affinity improvement beyond in vivo maturation. *Nat. Biotechnol.* 25: 1171–1176.
26. Sharp, K. A., and B. Honig. 1990. Electrostatic interactions in macromolecules: theory and applications. *Annu. Rev. Biophys. Biophys. Chem.* 19: 301–332.
27. Sinha, N., Y. Li, C. A. Lipschultz, and S. J. Smith-Gill. 2007. Understanding antibody-antigen associations by molecular dynamics simulations: detection of important intra- and inter-molecular salt bridges. *Cell Biochem. Biophys.* 47: 361–375.
28. Mallon, D. H., J. A. Bradley, P. J. Winn, C. J. Taylor, and V. Kosmoliaptsis. 2015. Three-dimensional structural modelling and calculation of electrostatic potentials of HLA Bw4 and Bw6 epitopes to explain the molecular basis for alloantibody binding: toward predicting HLA antigenicity and immunogenicity. *Transplantation* 99: 385–390.
29. Mallon, D. H., J. A. Bradley, C. J. Taylor, and V. Kosmoliaptsis. 2014. Structural and electrostatic analysis of HLA B-cell epitopes: inference on immunogenicity and prediction of humoral alloresponses. *Curr. Opin. Organ Transplant.* 19: 420–427.
30. Kosmoliaptsis, V., T. R. Dafforn, A. N. Chaudhry, D. J. Halsall, J. A. Bradley, and C. J. Taylor. 2011. High-resolution, three-dimensional modeling of human leukocyte antigen class I structure and surface electrostatic potential reveals the molecular basis for alloantibody binding epitopes. *Hum. Immunol.* 72: 1049–1059.
31. Kling, C., J. Steinmann, E. Westphal, J. Magez, and D. Kabelitz. 2006. Adverse effects of intradermal allogeneic lymphocyte immunotherapy: acute reactions and role of autoimmunity. *Hum. Reprod.* 21: 429–435.
32. Kling, C., J. Steinmann, B. Flesch, E. Westphal, and D. Kabelitz. 2006. Transfusion-related risks of intradermal allogeneic lymphocyte immunotherapy: single cases in a large cohort and review of the literature. *Am. J. Reprod. Immunol.* 56: 157–171.
33. Kling, C., A. Schmutzler, G. Wilke, J. Hedderich, and D. Kabelitz. 2008. Two-year outcome after recurrent implantation failure: prognostic factors and additional interventions. [Published erratum appears in 2018 *Arch. Gynecol. Obstet.* 298: 851.] *Arch. Gynecol. Obstet.* 278: 135–142.
34. Wellcome Trust Case Control Consortium (WTCCC). 2011. Dense genotyping identifies and localizes multiple common and rare variant association signals in celiac disease. *Nat. Genet.* 43: 1193–1201.
35. Dilthey, A., S. Leslie, L. Moutsianas, J. Shen, C. Cox, M. R. Nelson, and G. McVean. 2013. Multi-population classical HLA type imputation. *PLoS Comput. Biol.* 9: e1002877.
36. Jia, X., B. Han, S. Onengut-Gumuscu, W.-M. Chen, P. J. Concannon, S. S. Rich, S. Raychaudhuri, and P. I. W. de Bakker. 2013. Imputing amino acid polymorphisms in human leukocyte antigens. *PLoS One* 8: e64683.
37. Eswar, N., B. Webb, M. A. Marti-Renom, M. S. Madhusudhan, D. Eramian, M. Y. Shen, U. Pieper, and A. Sali. 2006. Comparative protein structure modeling using modeller. *Curr. Protoc. Bioinformatics* Chapter 5: Unit-5.6.
38. Hooft, R. W., G. Vriend, C. Sander, and E. E. Abola. 1996. Errors in protein structures. *Nature* 381: 272.
39. Laskowski, R. A., M. W. MacArthur, D. Moss, and J. M. Thornton. 1993. PROCHECK: a program to check the stereochemical quality of protein structures. *J. Appl. Cryst.* 26: 283–291.
40. Lüthy, R., J. U. Bowie, and D. Eisenberg. 1992. Assessment of protein models with three-dimensional profiles. *Nature* 356: 83–85.
41. Shen, M. Y., and A. Sali. 2006. Statistical potential for assessment and prediction of protein structures. *Protein Sci.* 15: 2507–2524.
42. Larkin, M. A., G. Blackshields, N. P. Brown, R. Chenna, P. A. McGettigan, H. McWilliam, F. Valentin, I. M. Wallace, A. Wilm, R. Lopez, et al. 2007. Clustal W and clustal X version 2.0. *Bioinformatics* 23: 2947–2948.

43. Olsson, M. H. M., C. R. Søndergaard, M. Rostkowski, and J. H. Jensen. 2011. PROPKA3: consistent treatment of internal and surface residues in empirical pKa predictions. *J. Chem. Theory Comput.* 7: 525–537.
44. Sitkoff, D., K. A. Sharp, and B. Honig. 1994. Accurate calculation of hydration free energies using macroscopic solvent models. *J. Phys. Chem.* 98: 1978–1988.
45. Dolinsky, T. J., J. E. Nielsen, J. A. McCammon, and N. A. Baker. 2004. PDB2PQR: an automated pipeline for the setup of Poisson-Boltzmann electrostatics calculations. *Nucleic Acids Res.* 32(Web Server issue): W665–7.
46. Callenberg, K. M., O. P. Choudhary, G. L. de Forest, D. W. Gohara, N. A. Baker, and M. Grabe. 2010. APBSmem: a graphical interface for electrostatic calculations at the membrane. *PLoS One* 5: e12722
47. Blomberg, N., R. R. Gabdoulline, M. Nilges, and R. C. Wade. 1999. Classification of protein sequences by homology modeling and quantitative analysis of electrostatic similarity. *Proteins* 37: 379–387.
48. Wade, R. C., R. R. Gabdoulline, and F. De Rienzo. 2001. Protein interaction property similarity analysis. *Int. J. Quantum Chem.* 83: 122–127.
49. Quebec IBD Genetics Consortium; International Inflammatory Bowel Disease Genetics Consortium; Australia and New Zealand IBDGC; United Kingdom IBDGC; Belgium IBD Genetics Consortium; Italian Group for IBD Genetic Consortium; NIDDK Inflammatory Bowel Disease Genetics Consortium; Wellcome Trust Case Control Consortium. 2015. High-density mapping of the MHC identifies a shared role for HLA-DRB1*01:03 in inflammatory bowel diseases and heterozygous advantage in ulcerative colitis. *Nat. Genet.* 47: 172–179.
50. Hodgkin, E. E., and W. G. Richards. 1987. Molecular similarity based on electrostatic potential and electric field. *Int. J. Quantum Chem.* 32(S14): 105–110.
51. R. Development Core Team. (2014). *R: A Language and Environment for Statistical Computing*. R Foundation for Statistical Computing, Vienna, Austria. http://www.R-project.org/.
52. Apps, R., Z. Meng, G. Q. Del Prete, J. D. Lifson, M. Zhou, and M. Carrington. 2015. Relative expression levels of the HLA class-I proteins in normal and HIV-infected cells. *J. Immunol.* 194: 3594–3600.
53. Thomas, R., C. L. Thio, R. Apps, Y. Qi, X. Gao, D. Marti, J. L. Stein, K. A. Soderberg, M. A. Moody, J. J. Goedert, et al. 2012. A novel variant marking HLA-DP expression levels predicts recovery from hepatitis B virus infection. *J. Virol.* 86: 6979–6985.
54. Petersdorf, E. W., M. Malkki, C. O'hUigin, M. Carrington, T. Gooley, M. D. Haagenson, M. M. Horowitz, S. R. Spellman, T. Wang, and P. Stevenson. 2015. High HLA-DP expression and graft-versus-host disease. *N. Engl. J. Med.* 373: 599–609.
55. Edwards, J. A., B. M. Durant, D. B. Jones, P. R. Evans, and J. L. Smith. 1986. Differential expression of HLA class II antigens in fetal human spleen: relationship of HLA-DP, DQ, and DR to immunoglobulin expression. *J. Immunol.* 137: 490–497.
56. Guardiola, J., and A. Maffei. 1993. Control of MHC class II gene expression in autoimmune, infectious, and neoplastic diseases. *Crit. Rev. Immunol.* 13: 247–268.
57. Tagliamacco, A., M. Cioni, P. Comoli, M. Ramondetta, C. Brambilla, A. Trivelli, A. Magnasco, R. Biticchi, I. Fontana, P. Dulbecco, et al. 2014. DQ molecules are the principal stimulators of de novo donor-specific antibodies in nonsensitized pediatric recipients receiving a first kidney transplant. *Transpl. Int.* 27: 667–673.
58. DeVos, J. M., A. O. Gaber, R. J. Knight, G. A. Land, W. N. Suki, L. W. Gaber, and S. J. Patel. 2012. Donor-specific HLA-DQ antibodies may contribute to poor graft outcome after renal transplantation. *Kidney Int.* 82: 598–604.
59. Willicombe, M., P. Brookes, R. Sergeant, E. Santos-Nunez, C. Steggar, J. Galliford, A. McLean, T. H. Cook, T. Cairns, C. Roufosse, and D. Taube. 2012. De novo DQ donor-specific antibodies are associated with a significant risk of antibody-mediated rejection and transplant glomerulopathy. *Transplantation* 94: 172–177.
60. Tikkanen, J. M., L. G. Singer, S. J. Kim, Y. Li, M. Binnie, C. Chaparro, C. W. Chow, T. Martinu, S. Azad, S. Keshavjee, and K. Tinckam. 2016. De novo DQ donor-specific antibodies are associated with chronic lung allograft dysfunction after lung transplantation. *Am. J. Respir. Crit. Care Med.* 194: 596–606.
61. Dieplinger, G., M. J. Everly, L. M. Rebellato, C. E. Haisch, K. P. Briley, P. Bolin, W. T. Kendrick, S. A. Kendrick, C. Morgan, R. C. Harland, and P. I. Terasaki. 2014. Changes in successive measures of de novo donor-specific anti-human leukocyte antigen antibodies intensity and the development of allograft dysfunction. *Transplantation* 98: 1097–1104.
62. Mujtaba, M. A., W. Goggins, A. Lobashevsky, A. A. Sharfuddin, M. S. Yaqub, D. P. Mishler, Z. Brahmi, N. Higgins, M. M. Milgrom, A. Diez, and T. Taber. 2011. The strength of donor-specific antibody is a more reliable predictor of antibody-mediated rejection than flow cytometry crossmatch analysis in desensitized kidney recipients. *Clin. Transplant.* 25: E96–E102.
63. Wiebe, C., T. E. Nevins, W. N. Robiner, W. Thomas, A. J. Matas, and P. W. Nickerson. 2015. The synergistic effect of class II HLA epitope-mismatch and nonadherence on acute rejection and graft survival. *Am. J. Transplant.* 15: 2197–2202.
64. Claas, F. H., M. K. Dankers, M. Oudshoorn, J. J. van Rood, A. Mulder, D. L. Roelen, R. J. Duquesnoy, and I. I. Doxiadis. 2005. Differential immunogenicity of HLA mismatches in clinical transplantation. *Transpl. Immunol.* 14: 187–191.
65. Copley, H. C., M. Elango, and V. Kosmoliaptsis. 2018. Assessment of human leukocyte antigen immunogenicity: current methods, challenges and opportunities. *Curr. Opin. Organ Transplant.* 23: 477–485.
66. Wiebe, C., V. Kosmoliaptsis, D. Pochinco, C. J. Taylor, and P. Nickerson. 2018. A comparison of HLA molecular mismatch methods to determine HLA immunogenicity. *Transplantation* 102: 1338–1343.
67. Nakamura, H. 1996. Roles of electrostatic interaction in proteins. *Q. Rev. Biophys.* 29: 1–90.
68. Sinha, N., and S. J. Smith-Gill. 2002. Electrostatics in protein binding and function. *Curr. Protein Pept. Sci.* 3: 601–614.
69. Schwickert, T. A., G. D. Victora, D. R. Fooksman, A. O. Kamphorst, M. R. Mugnier, A. D. Gitlin, M. L. Dustin, and M. C. Nussenzweig. 2011. A dynamic T cell-limited checkpoint regulates affinity-dependent B cell entry into the germinal center. *J. Exp. Med.* 208: 1243–1252.
70. Allen, C. D., T. Okada, H. L. Tang, and J. G. Cyster. 2007. Imaging of germinal center selection events during affinity maturation. *Science* 315: 528–531.
71. Kurosaki, T., K. Kometani, and W. Ise. 2015. Memory B cells. *Nat. Rev. Immunol.* 15: 149–159.
72. Tran, A., D. Fixler, R. Huang, T. Meza, C. Lacelle, and B. B. Das. 2016. Donor-specific HLA alloantibodies: impact on cardiac allograft vasculopathy, rejection, and survival after pediatric heart transplantation. *J. Heart Lung Transplant.* 35: 87–91.
73. Morrell, M. R., J. M. Pilewski, C. J. Gries, M. R. Pipeling, M. M. Crespo, C. R. Ensor, S. A. Yousem, J. D'Cunha, N. Shigemura, C. A. Bermudez, et al. 2014. De novo donor-specific HLA antibodies are associated with early and high-grade bronchiolitis obliterans syndrome and death after lung transplantation. *J. Heart Lung Transplant.* 33: 1288–1294.
74. Cheng, E. Y., M. J. Everly, H. Kaneku, N. Banuelos, L. J. Wozniak, R. S. Venick, E. A. Marcus, S. V. McDiarmid, R. W. Busuttil, P. I. Terasaki, and D. G. Farmer. 2017. Prevalence and clinical impact of donor-specific alloantibody among intestinal transplant recipients. *Transplantation* 101: 873–882.
75. Loupy, A., C. Lefaucheur, D. Vernerey, C. Prugger, J. P. Duong van Huyen, N. Mooney, C. Suberbielle, V. Frémeaux-Bacchi, A. Méjean, F. Desgrandchamps, et al. 2013. Complement-binding anti-HLA antibodies and kidney-allograft survival. *N. Engl. J. Med.* 369: 1215–1226.
76. Roux, A., I. Bendib Le Lan, S. Holifanjaniaina, K. A. Thomas, A. M. Hamid, C. Picard, D. Grenet, S. De Miranda, B. Douvry, L. Beaumont-Azuar, et al; Foch Lung Transplantation Group. 2016. Antibody-mediated rejection in lung transplantation: clinical outcomes and donor-specific antibody characteristics. *Am. J. Transplant.* 16: 1216–1228.
77. Mittal, S., S. L. Page, P. J. Friend, E. J. Sharples, and S. V. Fuggle. 2014. De novo donor-specific HLA antibodies: biomarkers of pancreas transplant failure. *Am. J. Transplant.* 14: 1664–1671.
78. Smith, J. D., N. R. Banner, I. M. Hamour, M. Ozawa, A. Goh, D. Robinson, P. I. Terasaki, and M. L. Rose. 2011. De novo donor HLA-specific antibodies after heart transplantation are an independent predictor of poor patient survival. *Am. J. Transplant.* 11: 312–319.
79. Fuller, T. C., and A. Fuller. 1999. The humoral immune response against an HLA class I allodeterminant correlates with the HLA-DR phenotype of the responder. *Transplantation* 68: 173–182.
80. Dankers, M. K., D. L. Roelen, N. J. Nagelkerke, P. de Lange, G. G. Persijn, I. I. Doxiadis, and F. H. Claas. 2004. The HLA-DR phenotype of the responder is predictive of humoral response against HLA class I antigens. *Hum. Immunol.* 65: 13–19.
81. Andreatta, M., E. Karosiene, M. Rasmussen, A. Stryhn, S. Buus, and M. Nielsen. 2015. Accurate pan-specific prediction of peptide-MHC class II binding affinity with improved binding core identification. *Immunogenetics* 67: 641–650.
82. Lachmann, N., M. Niemann, P. Reinke, K. Budde, D. Schmidt, F. Halleck, A. Pruß, C. Schönemann, E. Spierings, and O. Staeck. 2017. Donor-recipient matching based on predicted indirectly recognizable HLA epitopes independently predicts the incidence of de novo donor-specific HLA antibodies following renal transplantation. *Am. J. Transplant.* 17: 3076–3086.
83. Geneugelijk, K., G. Hönger, H. W. M. van Deutekom, K. A. Thus, C. Keşmir, I. Hösli, S. Schaub, and E. Spierings. 2015. Predicted indirectly recognizable HLA epitopes presented by HLA-DRB1 are related to HLA antibody formation during pregnancy. *Am. J. Transplant.* 15: 3112–3122.
84. Otten, H. G., J. J. Calis, C. Keşmir, A. D. van Zuilen, and E. Spierings. 2013. Predicted indirectly recognizable HLA epitopes presented by HLA-DR correlate with the de novo development of donor-specific HLA IgG antibodies after kidney transplantation. *Hum. Immunol.* 74: 290–296.
85. Roche, P. A., and K. Furuta. 2015. The ins and outs of MHC class II-mediated antigen processing and presentation. *Nat. Rev. Immunol.* 15: 203–216.
86. Wang, P., J. Sidney, Y. Kim, A. Sette, O. Lund, M. Nielsen, and B. Peters. 2010. Peptide binding predictions for HLA DR, DP and DQ molecules. *BMC Bioinformatics* 11: 568.
87. Wang, P., J. Sidney, C. Dow, B. Mothé, A. Sette, and B. Peters. 2008. A systematic assessment of MHC class II peptide binding predictions and evaluation of a consensus approach. *PLOS Comput. Biol.* 4: e1000048.
88. Agudelo, W. A., and M. E. Patarroyo. 2010. Quantum chemical analysis of MHC-peptide interactions for vaccine design. *Mini Rev. Med. Chem.* 10: 746–758.
89. Lubinski, J., V. J. Vrdoljak, K. D. Beaman, J. Y. Kwak, A. E. Beer, and A. Gilman-Sachs. 1993. Characterization of antibodies induced by paternal lymphocyte immunization in couples with recurrent spontaneous abortion. *J. Reprod. Immunol.* 24: 81–96.
90. Jolly, E. C., T. Key, H. Rasheed, H. Morgan, A. Butler, N. Pritchard, C. J. Taylor, and M. R. Clatworthy. 2012. Preformed donor HLA-DP-specific antibodies mediate acute and chronic antibody-mediated rejection following renal transplantation. *Am. J. Transplant.* 12: 2845–2848.
91. Mytilineos, J., A. Deufel, and G. Opelz. 1997. Clinical relevance of HLA-DPB locus matching for cadaver kidney retransplants: a report of the Collaborative transplant study. *Transplantation* 63: 1351–1354.
92. Schaub, S., G. Hönger, M. T. Koller, R. Liwski, and P. Amico. 2014. Determinants of C1q binding in the single antigen bead assay. *Transplantation* 98: 387–393.
93. Taylor, C. J., V. Kosmoliaptsis, J. Martin, G. Knighton, D. Mallon, J. A. Bradley, and S. Peacock. 2017. Technical limitations of the C1q single-antigen bead assay to detect complement binding HLA-specific antibodies. *Transplantation* 101: 1206–1214.
94. Wiebe, C., A. J. Gareau, D. Pochinco, I. W. Gibson, J. Ho, P. E. Birk, T. Blydt-Hansen, M. Karpinski, A. Goldberg, L. Storsley, et al. 2017. Evaluation of C1q status and titer of de novo donor-specific antibodies as predictors of allograft survival. *Am. J. Transplant.* 17: 703–711.